ISA Transactions 53 (2014) 1901–1909

Contents lists available at ScienceDirect

ISA Transactions

journal homepage: www.elsevier.com/locate/isatrans

Research Article

Generalized proportional integral control for periodic signals under active disturbance rejection approach

John Cortés-Romero, Germán A. Ramos, Horacio Coral-Enriquez *

Universidad Nacional de Colombia, Facultad de Ingeniería, Departamento de Ingeniería Eléctrica y Electrónica, Bogotá D.C., Colombia

ARTICLE INFO

Article history:
Received 2 April 2014
Received in revised form
25 June 2014
Accepted 3 July 2014
Available online 5 August 2014
This paper was recommended for publication by Dr. Jeff Pieper

Keywords:
Active disturbance rejection control
GPI control
Disturbance observers
Repetitive control
Periodic disturbances

ABSTRACT

Conventional repetitive control has proven to be an effective strategy to reject/track periodic signals with constant frequency; however, it shows poor performance in varying frequency applications. This paper proposes an active disturbance rejection methodology applied to a large class of uncertain flat systems for the tracking and rejection of periodic signals, in which the possibilities of the generalized proportional integral (GPI) observer-based control to address repetitive control problems are studied. In the proposed scheme, model uncertainties and external disturbances are lumped together in a general additive disturbance input that is estimated and rejected on-line. An illustrative case study of mechatronic nature is considered. Experimental results show that the proposed GPI observer-based control successfully rejects periodic disturbances even under varying speed conditions.

1. Introduction

Tracking and rejection of periodic signals is a subject of great research interest in control theory. It includes a wide range of engineering applications, some of them cover hard disk controllers [1], robotics [2], electronic inverters [3], active power filters [4], wind turbines [5], among others.

One approach that has been remarkably successful in the area is the iterative learning control (see [6]). Within this context, repetitive control (RC) emerges as a technique, based on the internal model principle (IMP), which has been very efficient in control applications that require tracking and/or rejection of periodic signals (see [7]). However, if the fundamental frequency of the periodic signal changes, it will cause that RC drastically loses its performance [8]. To allow RC to operate properly at varying frequency, some modifications are needed, such as frequency estimators [9], high order repetitive control [10] and variable sampling period [11]. But these modifications may result in very complex control systems.

With a rather different philosophy, a new control paradigm is established with the name of active disturbance rejection control (ADRC) (see [12–15]) where disturbances, unmodeled dynamics and parameter uncertainty are treated as a lumped disturbance signal. This unified disturbance signal is estimated on-line with a pre-defined level of approximation and then is canceled by a control law that is remarkably simple by making use of this estimate.

A well founded methodology within the scope of ADRC is the generalized proportional integral (GPI) control (see [16,17]). In the present work, the possibilities of GPI strategy under an ADRC approach for tracking and/or rejection of periodic signals for differentially flat system are analyzed. The GPI strategy is compared to a conventional RC, which is a specialized technique intended for handling this type of signals. The strategy shows to be effective at constant frequency as well as at varying frequency without any additional modification. In this way, the proposed controller does not need any frequency estimator or adaptive mechanism. Unlike other conventional ADRC based approaches, the work reported here proposes and recommends the use of a higher internal model in order to better approximate the periodic disturbance. The strategy is experimentally validated in a rotational mechatronic system, which entails a very large type of engineering applications. The implementation shows very good performance also in case of varying/uncertain frequency. The parameter selection is discussed and the tuning procedure has been described in detail. Finally, a robustness analysis is presented where performance and stability are studied.

The paper is organized as follows: Section 2 describes the conventional repetitive control strategy. Section 3 presents the GPI

* Corresponding author. Present address: Universidad Nacional de Colombia, Av. K30 No. 45-03, Edif. 411 Of. 203A, Bogotá, Colombia. Tel.: +57 1 3165000x11147.
E-mail addresses: jacortesr@unal.edu.co (J. Cortés-Romero), garamosf@unal.edu.co (G.A. Ramos), hacorale@unal.edu.co (H. Coral-Enriquez).

http://dx.doi.org/10.1016/j.isatra.2014.07.001
0019-0578/

technique, describing its design methodology. In Section 4, as a case study, a mechatronic system with periodic disturbances is considered. A comparison between the conventional strategy and the proposed GPI-based strategy is provided. The experimental results are presented in Section 5, where specific comparisons of performance for different velocity profiles are shown. Finally, Section 6 gives the conclusions and recommendations on the use of these strategies for periodic signal handling.

2. Conventional repetitive control strategy

The IMP establishes that in order to robustly track or reject a given signal, the model of the signal must be included in the control loop [18]. Following this principle, RC has been successfully used in the tracking/rejection of periodic signals [7]. It uses a periodic signal generator in the control loop:

$$G_{im}(s)=\frac{e^{(-T_p+T_h)s}H(s)}{1-e^{(-T_p+T_h)s}H(s)} \tag{1}$$

where $H(s)$ is a lowpass filter that limits the action of the controller in the high frequency range, T_p is the period of the signal and T_h is included to compensate for the phase of $H(s)$ at fundamental frequency; in this way $T_h=\arg(H(j\omega_1))T_p/(2\pi)$, being ω_1 the nominal fundamental frequency in rad/s. With $H(s)=1$, this internal model would provide infinite gain at the fundamental frequency $f=1/T_p$ and all its harmonics.

The *plug-in* structure shown in Fig. 1 is commonly used to add the internal model to the system. Thus, the internal model extends an existing control loop consisting of $G_c(s)$ and the plant $G_p(s)$, which defines the closed loop transfer function $G_o(s)=G_c(s)G_p(s)/(1+G_c(s)G_p(s))$. Additionally, in Fig. 1, the filter $G_x(s)$ is added to provide system stability.

Closed loop system stability of Fig. 1 is established under the following conditions [19]:

1. Closed loop without repetitive controller, i.e. $G_o(s)$, is stable.
2. $\|H(s)(1-G_x(s)G_o(s))\|_\infty<1$.

Condition 2 can be used as a design rule for filters $H(s)$ and $G_x(s)$. Usually, $H(s)$ is chosen to accomplish $\|H(s)\|_\infty=1$ and $G_x(s)$ is used to cancel out the phase of $G_o(s)$ in the frequency interval of interest [20,21]. Thus, for non-minimum phase systems:

$$G_x(s)=k_r(s+\alpha)^l/G_o(s), \tag{2}$$

where the term $(s+\alpha)^l$ is defined to provided a proper transfer function, being l and α the parameters that determine the frequency interval where $G_x(s)$ approximates to $1/G_o(s)$.

3. GPI observer-based control strategy

The key in ADRC is the use of an extended state observer (ESO) for on-line estimation of uncertainties and disturbances. In this paper a GPI observer is in charge of that estimation.

In the GPI methodology, the input-to-output system representation, which can be of linear or non-linear[1] nature, is viewed as a linear additive perturbed system in which only the order of integration of the system and the control input gain are considered to be relevant for the controller design.[2] The unified additive term in the input–output dynamics can be effectively estimated, in an approximate manner, by means of the GPI observer. The lumped time-varying disturbance effect is modeled as a time polynomial and embedded as an *internal model* in a GPI observer. With this information, the controller cancels the disturbance term and regulates the resulting linear system. Thus the underlying control problem is reduced to a simple linear feedback control task requiring knowledge of a reduced set of system parameters to be implemented.

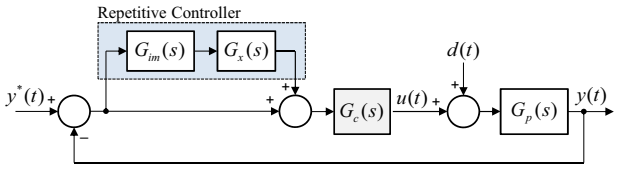

Fig. 1. *Plug-in* repetitive control structure.

3.1. Problem formulation

Consider the following scalar differentially flat system:

$$y^{(n)}(t)=\kappa u(t)+\phi(t,y(t),\dot{y}(t),\ldots,y^{(n-1)}(t))+\zeta(t), \tag{3}$$

we refer to κ as the control input gain of the system.[3] The term $\phi(t, y(t), \dot{y}(t), \ldots, y^{(n-1)}(t))$ will be addressed as the drift function which takes into account the remainder linear or non-linear dynamics, and $\zeta(t)$ represents the external disturbances. The unperturbed system, $\zeta(t)=0$, is flat, given that all variables in the system are expressed as differential functions of the flat output $y(t)$. Under the ADRC approach, the uncertain internal dynamics and the external disturbance are lumped in an unified additive disturbance input $\xi(t)$, regardless of any particular internal structure. As a result, the following simplified system can be defined:

$$y^{(n)}(t)=\kappa u(t)+\xi(t). \tag{4}$$

Then, the control objective is to drive the flat output $y(t)$ of the system (4) to track a given smooth reference trajectory $y^*(t)$, regardless of the unknown but uniformly bounded nature of the disturbance function $\xi(t)$.

Regarding the controlled system (4), we make the following assumptions:

(A1) The disturbance function $\xi(t)$ is completely unknown, while the control input gain κ is perfectly known.
(A2) Let m be a given integer. As a time function, the m-th time derivative of $\xi(t)$ is uniformly absolutely bounded. In other words, there exists a constant K_m so that $\sup_t|\xi^{(m)}(t)|\le K_m$.

Assumption A1 is made to ensure the independence of $\xi(t)$ from $u(t)$, thus, allowing a proper definition of the control law that will be proposed in Section 3.3. Furthermore, this assumption does not limit the application of the proposed controller since, as it will be shown in Section 4.2.5, the control system is robust against uncertainty in the parameter κ. On the other hand, assumption A2 is used to establish the existence of the solution of the differential equation (4). The work presented in [23] shows the necessity of this assumption and also proposes a relaxation where stepwise disturbances can be considered. Also, in [24] it is shown that $\xi^{(m)}(t)$ must be absolutely bounded almost everywhere otherwise the solutions, $y(t)$, for (4) do not exist, for any finite $u(t)$.

[1] The non-linear systems considered in GPI methodology are the non-linear differentially flat systems [22].

[2] In the multivariable case, the order of integration of the Kronecker subsystems and the control input gain matrix of the system.

[3] In a more general scope, the control input gain can be considered as a function $\psi(t,y(t))$.

3.2. GPI observer based approach

With reference to the simplified system (4), in order to propose a GPI observer for a related state and disturbance function estimation, it is considered that the internal model of the disturbance function $\xi(t)$ is approximated by $d^m\xi(t)/dt^m \approx 0$, at the observer stage. This model is embedded into the augmented model which is characterized by the following extended state vector: $x(t)=[x_1(t)\ x_2(t)\ \cdots\ x_{n+m}(t)]^T$ with $x_1(t)=y(t), x_2(t)=\dot{y}(t), \ldots, x_n(t)=y^{(n-1)}(t), x_{n+1}(t)=\xi(t), \ldots, x_{n+m}(t)=\xi^{(m-1)}(t)$, the augmented state space model is given by

$$\dot{x}(t)=Ax(t)+B\kappa u(t)+E\xi^{(m)}(t), \quad y(t)=Cx(t) \tag{5}$$

$$\text{with} \quad A=\begin{bmatrix} 0 & 1 & 0 & \cdots & 0 \\ 0 & 0 & 1 & & 0 \\ \vdots & & & \ddots & \\ 0 & 0 & 0 & \cdots & 1 \\ 0 & 0 & 0 & \cdots & 0 \end{bmatrix} \in \mathbb{R}^{(n+m)\times(n+m)}, \quad B=\begin{bmatrix} 0 \\ \vdots \\ 1 \ _{(n-\text{th position})} \\ \vdots \\ 0 \end{bmatrix} \in \mathbb{R}^{(n+m)\times 1}, \quad C=[1\ 0\ \cdots\ 0]\in\mathbb{R}^{1\times(n+m)}, \quad E=[0\ 0\ \cdots\ 1]^T \in \mathbb{R}^{(n+m)\times 1}.$$

Now, the GPI observer for the state $x(t)$ is proposed:

$$\dot{\hat{x}}(t)=A\hat{x}(t)+B\kappa u(t)+L(y(t)-\hat{y}(t)), \quad \hat{y}(t)=C\hat{x}(t) \tag{6}$$

where $\hat{x}(t)=[\hat{x}_1(t)\ \hat{x}_2(t)\ \cdots\ \hat{x}_{n+m}(t)]^T$ is the estimation state vector and $L=[l_{n+m-1}\ \cdots\ l_1\ l_0]^T$ is the observer gains vector.

The estimation error vector $\tilde{e}_x(t)=[\tilde{e}_{x1}(t)\ \tilde{e}_{x2}(t)\ \cdots\ \tilde{e}_{x(n+m)}(t)]^T$, defined as $\tilde{e}_x(t)=x(t)-\hat{x}(t)$, satisfies

$$\dot{\tilde{e}}_x(t)=(A-LC)\tilde{e}_x(t)+E\xi^{(m)}(t)=A_e\tilde{e}_x(t)+E\xi^{(m)}(t) \tag{7}$$

with $A_e\in\mathbb{R}^{(n+m)\times(n+m)}$ and its characteristic polynomial in the complex variable s is given by

$$p_{\tilde{e}_x}(s)=\det(sI-A_e)=s^{n+m}+l_{n+m-1}s^{n+m-1}+\cdots+l_1s+l_0. \tag{8}$$

Theorem 1. *Suppose all previous assumptions are valid. Let the coefficients, $l_{n+m-1}, \ldots, l_1$ and l_0 of the polynomial $p_{\tilde{e}_x}(s)$ be chosen so that all its roots are exhibited to the left of the complex plane $\mathbb{C}$. Then, the trajectories of the estimation errors: $\tilde{e}_{x1}(t), \tilde{e}_{x2}(t), \ldots, \tilde{e}_{x(n+m-1)}(t)$ and $\tilde{e}_{x(n+m)}(t)$ all globally converge to a small as desired neighborhood of zero where they remain ultimately bounded. Moreover, this ultimate bound can be adjusted by a suitable selection of the observer gains $l_{n+m-1}, \ldots, l_1$ and l_0.*

Proof. See Appendix A

3.3. The disturbance canceling linearizing controller

The controller is designed in order to set, in a dominantly way, a desired trajectory tracking error characteristic polynomial. To do so, the control law is compound by:

- A feed forward term, for the cases when the flat-output reference trajectory is a priori available.
- Linear estimated state feedback weighted by controller gains, with estimates provided by the GPI observer.
- A disturbance rejection term, which is basically the disturbance estimation also provided by the GPI observer.

With respect to the system (4), the GPI observer-based control for trajectory tracking is

$$u(t)=\frac{1}{\kappa}\left[[y^*(t)]^{(n)}-\sum_{k=0}^{n-1}\gamma_k(\hat{x}_{k+1}(t)-[y^*(t)]^{(k)})-\hat{x}_{n+1}(t)\right] \tag{9}$$

with the set of coefficients $\{\gamma_0, \ldots, \gamma_{n-1}\}$ chosen so that $p_c(s)=s^n+\gamma_{n-1}s^{n-1}+\cdots+\gamma_0$ exhibits all its roots in the left half of $\mathbb{C}$. The closed loop output tracking error, $e_y(t)=y(t)-y^*(t)$, is governed by

$$e_y^{(n)}(t)+\gamma_{n-1}e_y^{(n-1)}(t)+\cdots+\gamma_0e_y(t)=(\xi(t)-\hat{x}_{n+1}(t))+\sum_{k=0}^{n-1}\gamma_k\tilde{e}_{x_{k+1}}(t). \tag{10}$$

Theorem 2. *The disturbance rejection output feedback controller (9) drives the trajectory of the controlled system output error $e_y(t)$ towards a small as desired vicinity of zero, provided the set of coefficients $\{\gamma_0, \ldots, \gamma_{n-1}\}$ are properly chosen so that $p_c(s)$ is a Hurwitz polynomial with roots to the left of the imaginary axis in $\mathbb{C}$.*

Proof. See Appendix B.

4. Case study

The system used for the experimental validation of the proposed control strategy is a mechatronic system affected by nonlinear periodic disturbances. It consists of a Pulse Width Modulation (PWM) electronic amplifier, a DC motor, a 500 Pulses Per

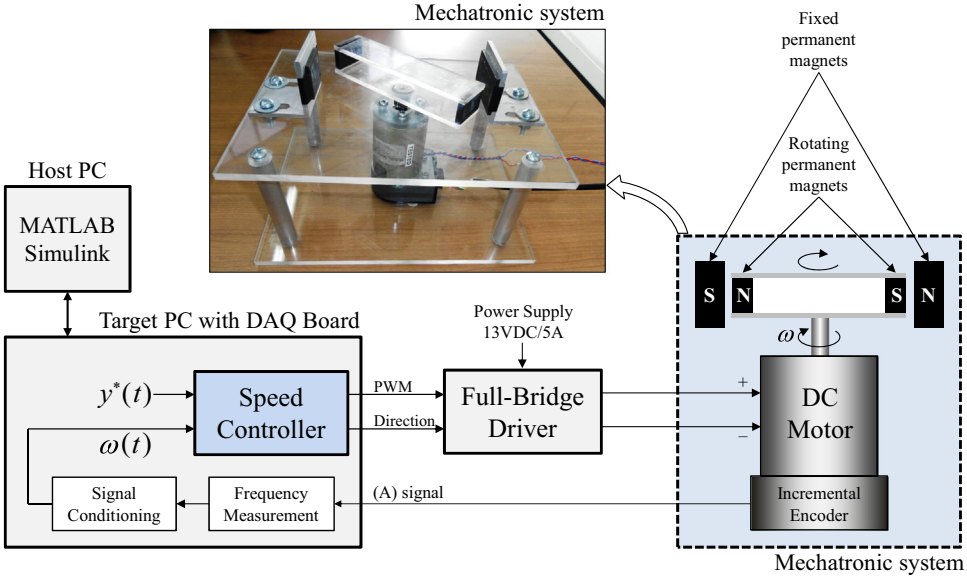

Fig. 2. General scheme and experimental setup of the case study.

Revolution (PPR) incremental encoder and a magnetic setup that generates a periodic torque under constant angular speed. This disturbance torque applied to the plant is a non-linear function of the angular position. Hence, the control objective is to regulate the angular speed of the motor to a desired value despite of the periodic torque disturbance. A detailed scheme of the mechatronic system, control loop and the experimental setup can be observed in Fig. 2. The reader is encouraged to read [25] for a more detailed explanation of this system (roto-magnet plant).

A dynamic model of the plant can be described as

$$\frac{d\omega(t)}{dt} = -\frac{k_i k_b}{JR_a}\omega(t) - \frac{B}{J}\omega(t) + \frac{2\pi k_i k_{pwm}}{JR_a}u(t) - \frac{2\pi}{J}\tau_d(t,\theta) \tag{11}$$

where $\omega(t)$ is the angular speed of the motor in rev/s, $u(t)$ is the control input in PWM percentage with range $[-100, 100]$, $k_{pwm} = 0.13$ V/% is the conversion constant from PWM percentage to volts, k_i is the torque constant, k_b is the back-emf constant, R_a is the armature resistance, J is the rotor inertia, B is the viscous-friction coefficient, and $\tau_d(t,\theta)$ is the disturbance torque, which in this case is the non-linear periodic torque produced by the magnetic setup.

From a simple experimental open-loop step response of the mechatronic system (free of periodic torque), the transfer function of the plant was identified as $G_p(s) = \Omega(s)/U(s) = 1.432/(s+1.613)$, then $(2\pi k_i k_{pwm}/JR_a) = 1.432$ and $((k_i k_b/JR_a)+(B/J)) = 1.613$.

Furthermore, since the magnetic setup of the mechatronic system is composed by two rotating magnets and two fixed magnets, the disturbance torque obeys the following non-linear function [26]:

$$\tau_d(t,\theta) = \sum_{i=1}^{2}\sum_{j=1}^{2} q_{m_i} m_j \tau_p(\theta + \theta_{i,j}, r_i, x_j) \tag{12}$$

with

$$\tau_p(\theta, r, x) = \frac{e}{m}(\sin(\rho)B_d + \cos(\rho)B_\alpha)$$

$$\rho = \arctan(r\ \sin(\theta), r\ \cos(\theta) - x) - \theta$$

$$B_d = \frac{\mu_0 m\ \cos(\arctan(r\ \sin(\theta), r\ \cos(\theta) - x))}{2\pi(-2r\ \cos\ (\theta)x + x^2 + r^2)^{3/2}}$$

$$B_\alpha = \frac{\mu_0 m\ \sin(\arctan(r\ \sin(\theta), r\ \cos(\theta) - x))}{4\pi(-2r\ \cos(\theta)x + x^2 + r^2)^{3/2}}$$

where, $\theta(t)$ is the angular position of the motor in rad, q_{m_i} is the magnetic intensity of the pole for the i-th moving magnet, m_j is the magnetic torque for the j-th fixed magnet, r_i is the distance between the i-th moving magnet and its rotation axis, x_j is the distance between the j-th fixed magnet and its rotation axis, $\theta_{i,j}$ is the relative position of the i-th moving magnet respect to the j-th fixed magnet, e is the thickness of each moving magnet, and μ_0 is the magnetic constant. For simulation purposes we use $\mu_0 = 4\pi \times 10^{-7}$ N A^{-2}, $e = 0.004$ m, $r_1 = 0.05$ m, $r_2 = 0.05$ m, $x_1 = 0.055$ m, $x_2 = 0.055$ m, $\theta_{11} = 0$ rad, $\theta_{12} = \pi$ rad, $\theta_{21} = \pi$ rad, $\theta_{22} = 0$ rad.

4.1. Repetitive control

RC is designed for a nominal frequency of $f = 4$ Hz corresponding to the system nominal speed. Thus, period $T_p = 1/4$ s and $T_h = 0.001$ s define the delay term in (1). The low-pass filter is selected as $H(s) = 1/(0.001s+1)$.

The selection of $G_c(s) = 5 + 29/s$ defines the closed loop without RC as $G_o(s) = (7.161s + 41.54)/(s^2 + 8.774s + 41.54)$. This allows the selection of filter $G_x(s)$ based on Eq. (2), with $l = 2$, $k_r = 0.3$ and $\alpha = 1000$. It is important to note that with this parameter selection, stability conditions of Section 2 hold.

4.2. GPI observer-based control

By considering the mechanical model of the motor (11) and its disturbance torque model (12), the system can be described as

$$\dot{x}_1(t) = \kappa u(t) + \xi(t) \tag{13}$$

where $x_1(t) = \omega(t)$, $\kappa = 2\pi k_i k_{pwm}/JR_a$, and $\xi(t) = -((k_i k_b/JR_a) + (B/J))\omega(t) - (2\pi/J)\tau_d(t,\theta) + \kappa\zeta(t)$ is considered as the disturbance signal to be actively rejected. $\zeta(t)$ represents external disturbances at the input of the plant and other unmodeled dynamics (e.g. electrical model), nonlinearities (e.g. coulomb and static friction) or uncertainty of the system (e.g. parameter variations).

4.2.1. Degree of approximation of the disturbance internal model

Following the design procedure proposed in Section 3, a degree of approximation of the disturbance internal model must be defined. Here, we discuss this topic and provide some guidelines to define it.

It is usual to select a first order approximation mainly because the disturbances are taken locally as additive constant signals or model uncertainties/nonlinearities. In this way, several authors have applied first order disturbance model approximation to different areas, for example: Professor C.D. Johnson used it to model wind speed disturbances in a wind turbine operating in region 3 [27], Freidovich and Khalil [28] used it to estimate the model uncertainty and disturbance on a nonlinear system, Gao and Zhao also used a first

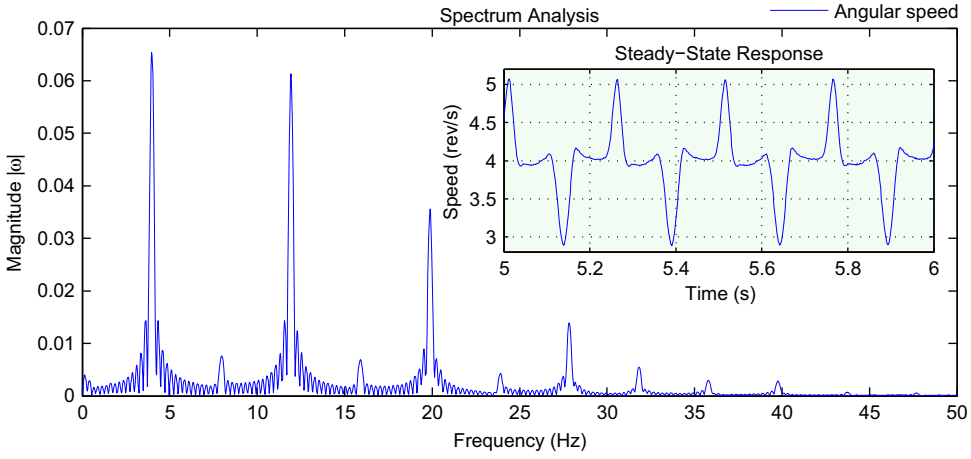

Fig. 3. Experimental open-loop speed response at nominal speed with periodic torque.

order internal model disturbance approximation to estimate the resonance in two-inertia systems [29].

Nevertheless, the disturbance internal model ($d^m\xi(t)/dt^m \approx 0$) is a more generalized extension and representation of the disturbance signal which provides extra information and increases the ability to track different types of disturbances. For example, $m=2$ allows local convergence to a disturbance with local constant derivative, $m=3$ allows local convergence to a disturbance with local constant acceleration, etc. Therefore, we can define the degree of approximation of the disturbance internal model by analyzing the complexity of the signal.

Notice that in order to obtain a good performance using a low order approximation (e.g. $d\xi(t)/dt \approx 0$) it would be necessary to design a high bandwidth observer. Of course, in those cases, the observer could give noisy estimations in practical applications.

In this case study, we determine the complexity of the disturbance torque applied to the plant by analyzing its effects on the open-loop response. Fig. 3 shows the experimental open-loop angular speed response which gives an idea of the complexity of the periodic disturbance torque. For this example, it is easy to know that a first or even a second degree of approximation is quite low because of the evident complex waveform of the signal. So, we decided to define the internal model approximation of the disturbance as $d^6\xi(t)/dt^6 \approx 0$. This will allow tuning the GPI observer with low-medium bandwidth.

4.2.2. GPI observer

According to the methodology proposed in Section 3.2, a GPI observer can be formulated based on the simplified system (13) and the approximation of the disturbance internal model, $d^6\xi(t)/dt^6 \approx 0$:

$$\dot{\hat{x}}(t) = A\hat{x}(t) + B\kappa u(t) + L(\omega(t) - \hat{\omega}(t)), \quad \hat{\omega}(t) = C\hat{x}(t) \tag{14}$$

with $\hat{x}(t) = [\hat{x}_1(t)\ \hat{x}_2(t)\ \hat{x}_3(t)\ \hat{x}_4(t)\hat{x}_5(t)\ \hat{x}_6(t)\hat{x}_7(t)]^T$, A a 7×7-matrix according to (5), $B = [1\ 0\ 0\ 0\ 0\ 0\ 0]^T$, $C = [1\ 0\ 0\ 0\ 0\ 0\ 0]$ and $L = [l_6\ l_5\ l_4\ l_3\ l_2\ l_1\ l_0]^T$; where, $\hat{x}_1(t)$ and $\hat{x}_2(t)$ are the estimated versions of $x_1(t)$ and $\xi(t)$, respectively.

As stated in Section 3.2, the dynamics of the estimation error vector of the GPI observer is dominated by the eigenvalues of $(A-LC)$. Thus, an appropriate choice of the observer gain $L = [l_6\ l_5\ l_4\ l_3\ l_2\ l_1\ l_0]^T$ placing the roots of the characteristic polynomial (see Eq. (8)):

$$\det(sI-(A-LC)) = s^7 + l_6 s^6 + l_5 s^5 + l_4 s^4 + l_3 s^3 + l_2 s^2 + l_1 s + l_0 \tag{15}$$

deep into the left half of the complex plane, renders an asymptotically, exponentially and decreasing estimation error.

4.2.3. Tuning of the GPI observer

The observer parameters $\{l_6, l_5, l_4, l_3, l_2, l_1, l_0\}$ are chosen using the methodology proposed by Kim et al. [30], who introduce the use of the characteristic ratio assignment to establish a desired well damped transient response of a LTI control system. This methodology is described in the following [30].

Consider a characteristic polynomial $A(s)$ of the form: $A(s) = a_n s^n + a_{n-1}s^{n-1} + \cdots + a_1 s + a_0$ with $a_i > 0$. Then, $A(s)$ is Hurwitz if the following two conditions hold:

$$\alpha_1 > 2, \tag{16}$$

$$\alpha_k = \alpha_1 \cdot \frac{\sin\left(\frac{\pi k}{n}\right) + \sin\left(\frac{\pi}{n}\right)}{2\sin\left(\frac{\pi k}{n}\right)}, \quad k = 2, 3, \ldots, (n-1), \tag{17}$$

with α_i the characteristic ratios of $A(s)$.

Thus, the all-pole stable characteristic polynomial $A(s)$ can be characterized by adjusting a single parameter $\alpha_1 > 2$ to achieve the desired damping. Then, the coefficients a_i of the polynomial $A(s)$ are calculated as follows:

$$a_1 = \tau a_0, \quad \text{for arbitrary } \tau > 0, \quad a_0 > 0$$

$$a_i = \frac{\tau^i a_0}{\alpha_{i-1}\alpha_{i-2}^2\alpha_{i-3}^3\cdots\alpha_1^{i-1}}, \quad \text{for } i = 2, 3, \ldots, n. \tag{18}$$

Finally, the parameters of the GPI observer are computed as

$$l_j = \left(\frac{a_j}{a_n}\right), \quad \text{for } j = 0, 1, 2, \ldots, (n-1). \tag{19}$$

The selection of the roots of the estimation error characteristic polynomial affects the bandwidth of the GPI observer and also the influence of measurement noises on the estimations. Therefore, GPI observers are usually tuned in a compromise between disturbance estimation performance (set by the internal model approximation degree) and noise sensitivity.

In the case study, we define $\tau = 0.15$ to establish a dominant generalized time constant with low bandwidth (≈ 10 rad/s), and $\alpha_1 = 3.2$ to maintain a well damped response (at least twice the distance between consecutive poles). These parameters allow the estimation error dynamics of the GPI observer to dominantly behave according to the following roots: [−12.2, −27.7, −59, −123, −255, −544, −1240].

4.2.4. Control law design

Once the estimations of the disturbance signal and the system states are available, a GPI observer-based control law is set following the results of Section 3.3:

$$u(t) = \frac{1}{\kappa}[\dot{y}^*(t) - \gamma(\hat{x}_1(t) - y^*(t)) - \hat{x}_2(t)]. \tag{20}$$

Replacing the control law (20) into the open-loop system (13), the closed loop tracking error dynamics $e_y(t) = y(t) - y^*(t)$ of the control system is governed by

$$\dot{e}_y(t) + \gamma e_y(t) = \gamma\underbrace{(y(t) - \hat{y}(t))}_{\tilde{e}_{x1}(t)} + \underbrace{(\xi(t) - \hat{\xi}(t))}_{\tilde{e}_{x2}(t)}. \tag{21}$$

Then, assuming that the estimation errors on right-hand side of Eq. (21) are close to zero (see Theorem 1), the closed-loop tracking error dynamics is dominantly governed by $e_y(t)(s+\gamma) \approx 0$. Therefore, we defined $\gamma = 8$ in order to set a settling time of 0.5 s in the transient response of the tracking error. This objective can be verified in Fig. 7, which shows the experimental transient response of the tracking error due to a setpoint step change.

Other techniques could be applied to tune the observer or controller parameters. A technique based on the extended symmetrical optimum method could be adapted in order to guarantee the robust stability of the closed-loop system with respect to parametric variations in the plant [31]. Other tuning methodologies based on H_∞ optimizations to guarantee stability and performance properties could be considered, the case of H_∞ LPV schemes [32] or H_∞ based on model matching schemes [33] may permit better tradeoff between robustness and performance. This will lead to another path of research outside of the aim of this paper.

4.2.5. Robustness analysis

In order to verify robustness and performance of the proposed controller, two analysis are made: (a) modify κ in the controller and evaluate closed-loop performance using the nominal plant, and (b) quantify the robustness of the proposed controller under parametric uncertainty in the plant.

For the first case, a strong variation in κ is considered: $\kappa \in \{0.1, 0.6, 1.432, 2.2, 3\}$. Observe that $\kappa = 1.432$ is the nominal value of the parameter. Thus, each controller is assessed in closed-loop by means of a step response in setpoint and an Integral of Square Error (ISE) index. Fig. 4 (right) shows the evolution in time of the ISE index under different values of κ. The plots show that

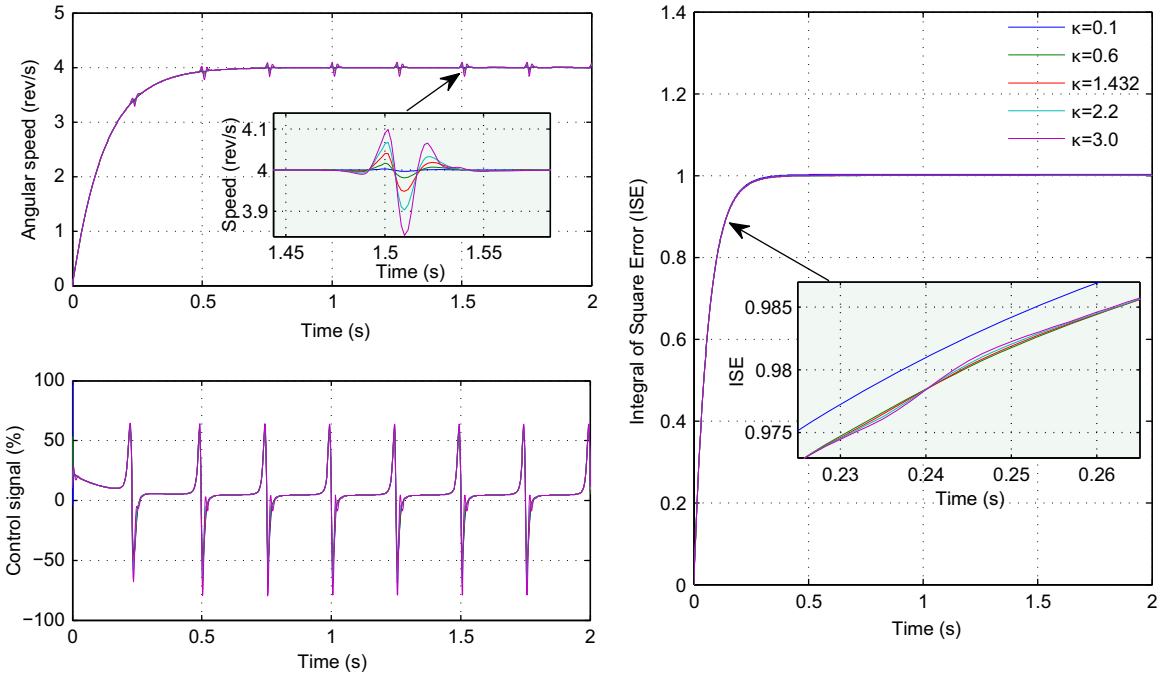

Fig. 4. Closed-loop transient response and disturbance rejection under variations of κ in the proposed controller.

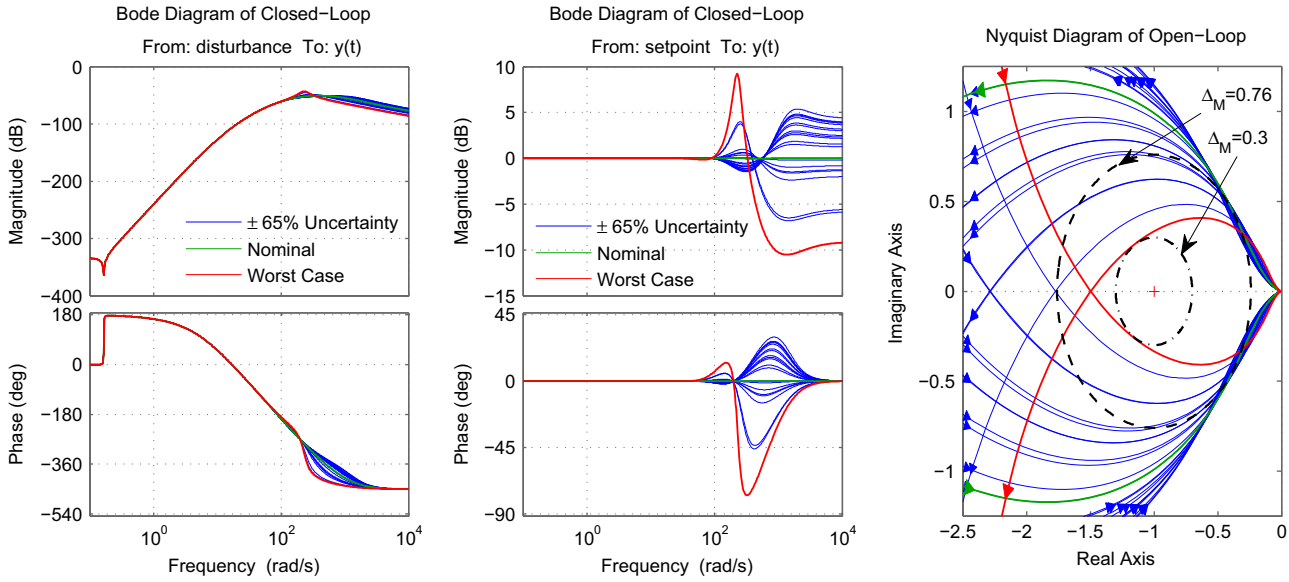

Fig. 5. Closed-loop frequency response and robustness analysis of the proposed controller. (For interpretation of the references to color in this figure caption, the reader is referred to the web version of this article.)

the proposed control system can handle such variations in κ without much degradation in the transient response. However, Fig. 4 (left) also shows that disturbance rejection performance is degraded when κ is greater than its nominal value.

For the second case, robustness of the control system is verified through Nyquist plots of the open-loop control system by measuring the modulus margin Δ_M. This analysis is carried out for a $\pm 65\%$ of uncertainty in each parameter of the plant. Fig. 5 details the Nyquist plots of the control system and reveals that the modulus margin in the nominal case (green) is $\Delta_M = 0.76$ and for the worst case (red) the modulus margin is $\Delta_M = 0.3$; this demonstrates robust stability.[4] In addition, closed-loop performance of the control system can be verified in the Bode diagrams of Fig. 5. These plots show the nominal frequency response, the frequency response with $\pm 65\%$ of uncertainty in each parameter of the plant, and the frequency response in the worst case.

5. Experimental results

In this section we show the experiments that were carried out to assess the performance of the proposed GPI observer-based controller against a conventional repetitive controller both applied to a mechatronic system affected by periodic disturbances. Two different operation cases are exposed and analyzed: a constant-speed profile and a variable-speed profile.

[4] A margin modulus $\Delta_M > 0.5$ is considered to be a good stability margin [34].

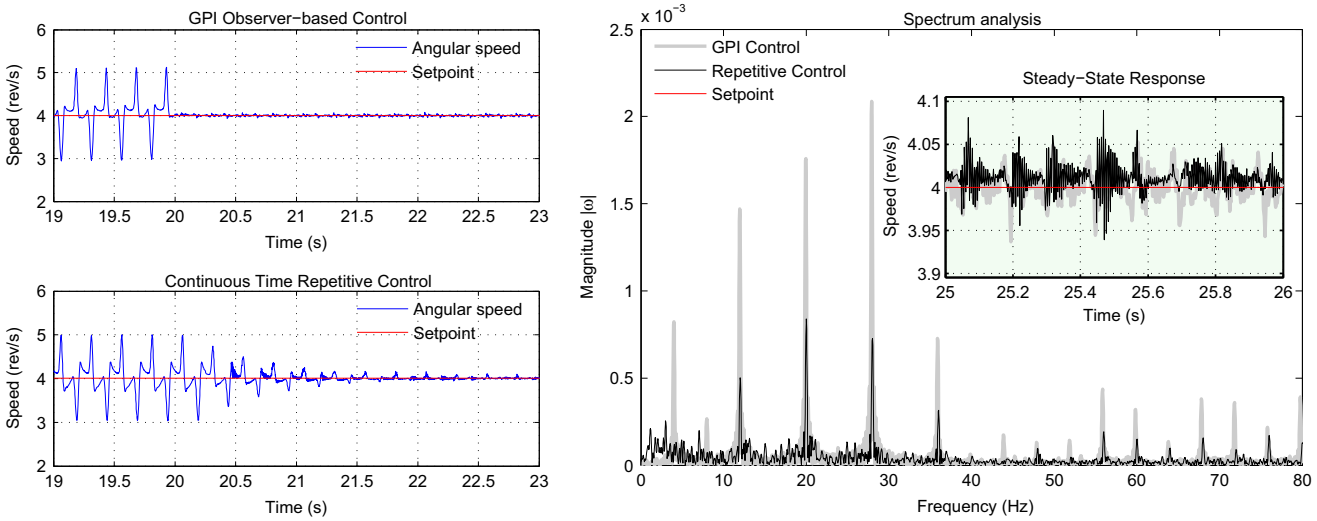

Fig. 6. Experimental response of the control systems using fixed setpoint at 4 rev/s. Each controller is activated from $t=20$ s.

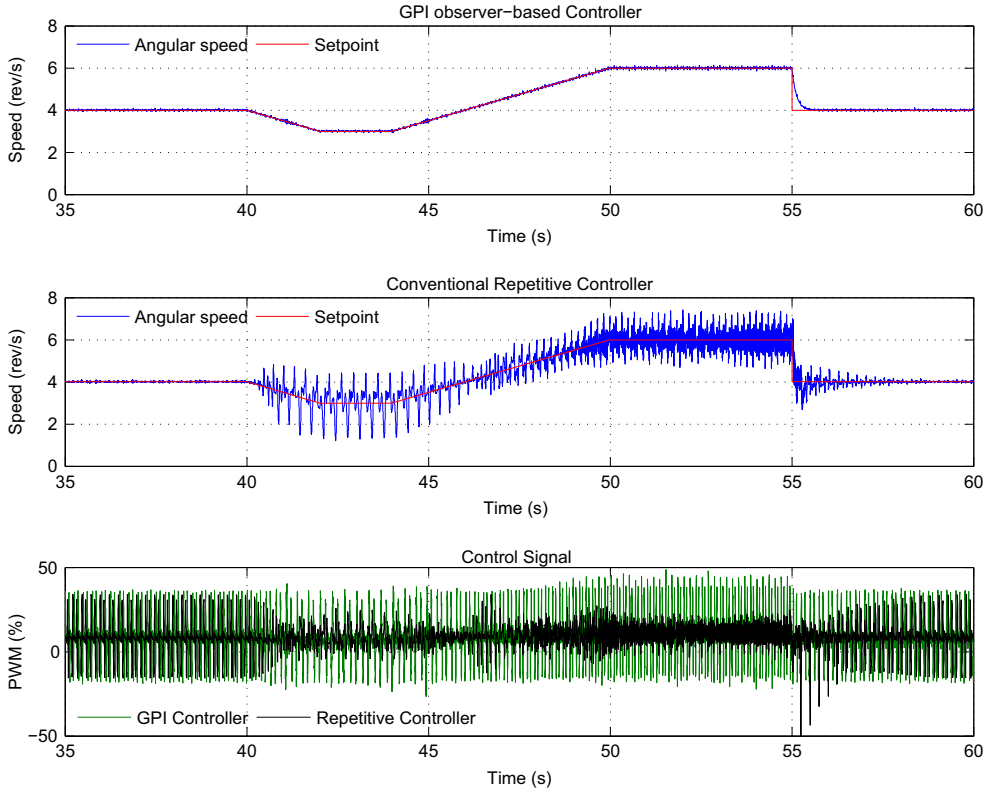

Fig. 7. Experimental response of the control systems using variable-speed setpoint.

5.1. Implementation issues

The connection between the mechatronic system and each controller was performed by a National Instruments PCI-6024E data acquisition card (see Fig. 2). A PWM output working at 20 kHz was used to command the dc-motor full-bridge driver and a counter input was used to read the frequency of the encoder's output.

The proposed strategy was implemented in a MATLAB – xPC Target environment on a computer equipped with a Pentium D processor. A discrete implementation of the control law (20) and the observer (14) is found by the discrete realization of the continuous time functions employing a selected integration method. In this case study, we used the Euler integration method with a sampling period of 0.1 ms. In addition, the reference signal derivatives needed to construct the control law (20) were pre-calculated before carrying out the implementation.

5.2. Constant-speed profile

Fig. 3 shows the open-loop system speed response in steady state obtained at a nominal speed of 4 rev/s. The harmonic content of the response is also shown. It is observed that the angular speed is affected by the disturbance in $\pm 25\%$. Fig. 6 shows the experimental results of the control systems under evaluation using a constant setpoint of 4 rev/s. It is shown that both control strategies are effective in rejecting the periodic disturbance at the nominal speed (tracking error being less than $\pm 1.25\%$).

The spectral content of the steady-state angular speed response for each control strategy is also shown in Fig. 6. It is noted that an effective rejection of the periodic disturbance has been done by both control strategies. The fundamental frequency of the disturbance and its main harmonics have been successfully attenuated. RC shows a better disturbance rejection at nominal speed; however, GPI control shows comparable performance by using a lower-order controller.

5.3. Variable-speed profile

In this case, the control systems use a variable-setpoint profile. Fig. 7 shows the experimental results of the control systems. The plots clearly show that RC is not capable of handling periodic disturbances outside of the nominal speed. On the other hand, GPI observer-based control achieved significant rejection of the periodic disturbance operating at variable-speed. The figure also shows, for $t \geq 55$, that the proposed controller performs a clear desired transient response with no visible disturbances. Experiments show a better tracking error performance at low speeds; however, at higher speeds, the tracking error performance is degraded because the disturbance involves harmonic components at higher frequencies.

6. Conclusions

In this paper, we test the GPI control capabilities for rejection/tracking of periodic signals. Both control strategies considered in this assessment provide comparable performance at the rated speed of operation. In the comparisons with respect to the speed variation (variable frequency), GPI control exhibits a notable advantage in terms of performance as can be evidenced in the obtained tracking error. The repetitive control strategy refers an important performance degradation under changes of the frequency of the disturbance input. This problem can be compensated using adaptive methods or higher order internal model schemes with a consequent increased complexity. On the other hand, the GPI observer based control strategy maintains a simple structure without adaptive mechanisms.

Appendix A. Proof of Theorem 1

Proof. The eigenvalues of A_e can be placed as desired by a proper selection of the design parameters $l_{n+m-1},\ldots,l_0$. The following discussions are all based on the fact that A_e is Hurwitz. For purposes of analysis of ultimate boundedness, transfer functions are used since the initial conditions do not affect the corresponding steady-state behavior. Thus, the following transfer functions associated with the estimation errors and the disturbance input $\xi^{(m)}(t)$, hereafter denoted as $\xi_m(t)$, are considered:

$$G_1(s) := \frac{\tilde{e}_{x_1}(s)}{\xi_m(s)} = \frac{1}{s^{n+m}+l_{n+m-1}s^{n+m-1}+\cdots+l_1 s+l_0} \tag{A.1}$$

$$G_2(s) := \frac{\tilde{e}_{x_2}(s)}{\xi_m(s)} = \frac{s+l_{n+m-1}}{s^{n+m}+l_{n+m-1}s^{n+m-1}+\cdots+l_1 s+l_0} \tag{A.2}$$

$$\vdots$$

$$G_{n+m}(s) := \frac{\tilde{e}_{x_{(n+m)}}(s)}{\xi_m(s)} = \frac{s^{n+m-1}+l_{n+m-1}s^{n+m-2}+\cdots+l_1}{s^{n+m}+l_{n+m-1}s^{n+m-1}+\cdots+l_1 s+l_0}. \tag{A.3}$$

Provided that A_e has r different eigenvalues with $\mathrm{Re}\{\lambda_i\}<0$, $i=1,\ldots,r$, (where n_i is the multiplicity of λ_i) in order to analyze the j-th estimation error $\tilde{e}_{x_j}(t)$, we consider the transfer function:

$$G_j(s) := \frac{\tilde{e}_{x_j}(s)}{\xi_m(s)} = \frac{s^{j-1}+l_{n+m-1}s^{j-2}+\cdots+l_{n+m-j+1}}{s^{n+m}+l_{n+m-1}s^{n+m-1}+\cdots+l_1 s+l_0}. \tag{A.4}$$

Expanding in partial fractions the transfer function:

$$G_j(s) = \sum_{i=1}^{r}\sum_{k=1}^{n_i}\frac{c_{ik}}{(s-\lambda_i)^k}. \tag{A.5}$$

The impulse response of (A.5) in time domain is given as follows:

$$g_j(t) = \sum_{i=1}^{r}\sum_{k=1}^{n_i}\frac{c_{ik}}{(k-1)!}t^{k-1}e^{\lambda_i t}. \tag{A.6}$$

It is important to note that the coefficients c_{ik} are dependent on the eigenvalues of A_e.

Regarding (A.4), the solution for $\tilde{e}_{x_j}(t)$ is given by

$$\tilde{e}_{x_j}(t) = \int_0^t g_j(\tau)\xi_m(t-\tau)\,d\tau \tag{A.7}$$

then

$$|\tilde{e}_{x_j}(t)| = \left|\int_0^t g_j(\tau)\xi_m(t-\tau)\,d\tau\right| \leq \int_0^t |g_j(\tau)\xi_m(t-\tau)|\,d\tau = \int_0^t |g_j(\tau)||\xi_m(t-\tau)|\,d\tau$$

using Assumption (A.2) and (A.6) follows that

$$\int_0^t |g_j(\tau)||\xi_m(t-\tau)|\,d\tau \leq K_m\int_0^t |g_j(\tau)|\,d\tau = K_m\int_0^t \left|\sum_{i=1}^{r}\sum_{k=1}^{n_i}\frac{c_{ik}}{(k-1)!}\tau^{k-1}e^{\lambda_i\tau}\right|d\tau$$

$$\leq K_m\sum_{i=1}^{r}\sum_{k=1}^{n_i}|c_{ik}|\int_0^t\frac{\tau^{k-1}}{(k-1)!}|e^{\lambda_i\tau}|\,d\tau.$$

Setting $\lambda_i = -\sigma_i + j\omega_{di}$, with $\sigma_i>0$, one obtains $|e^{\lambda_i\tau}| = |e^{-\sigma_i\tau+j\omega_{di}\tau}| \leq |e^{-\sigma_i\tau}||e^{j\omega_{di}\tau}| = |e^{-\sigma_i\tau}| = e^{-\sigma_i\tau}$, and using the following result:[5]

$$\lim_{t\to\infty}\int_0^t\frac{\tau^{k-1}}{(k-1)!}e^{-\sigma_i\tau}\,d\tau = \frac{1}{\sigma_i^k} \tag{A.8}$$

we have

$$\lim_{t\to\infty}|\tilde{e}_{x_j}(t)| \leq K_m\sum_{i=1}^{r}\sum_{k=1}^{n_i}|c_{ik}|\frac{1}{\sigma_i^k} \tag{A.9}$$

therefore $\tilde{e}_{x_j}(t)$, with $j=1,\ldots,n+m$, is bounded and the ultimate bound depends on the real part of the selected eigenvalues.

It is important to determine the effect of coefficients c_{ik} in the bound (A.9), but it can be a complicated analysis for the general case, for this reason we prefer to perform an analysis of a simple case when $r=1$, with $n_1=n+m$ real repeated eigenvalues. Under this case: $G_1(s)=\frac{c_{1n_1}}{(s-\lambda_1)^{n_1}}$; $c_{1n_1}=1$; $g_j(t)=\frac{1}{(n_1-1)!}t^{(n_1-1)}e^{\lambda_1 t}$ and using (A.8) we have

$$\lim_{t\to\infty}|\tilde{e}_{x_1}(t)| \leq K_m\frac{1}{|\lambda_1|^{n_1}}. \tag{A.10}$$

For other estimation errors under the same case (repeated eigenvalue λ_1):

$$G_j(s) = \sum_{k=1}^{n_1}\frac{c_{1k}}{(s-\lambda_1)^k}. \tag{A.11}$$

The c_{ik} coefficients can be determined finding the residues corresponding to the partial fraction expansion (A.11),

$$c_{1k} = \frac{1}{(n_1-k)!}\frac{d^{n_1-k}}{ds^{n_1-k}}\left\{s^{j-1}+l_{n+m-1}s^{j-2}+\cdots+l_{n+m-j+1}\right\}\Big|_{s=\lambda_1} \tag{A.12}$$

in terms of a $|\lambda_1|-$order we have that $|c_{1k}| = O(|\lambda_1|^{j-1-n_1+k})$, with O the order function. According to (A.9) we have

$$\lim_{t\to\infty}|\tilde{e}_{x_j}(t)| \leq K_m\sum_{k=1}^{n_1}|c_{1k}|\frac{1}{|\lambda_1|^k}. \tag{A.13}$$

Let us see the order of (A.13):

$$O\left(|c_{1k}|\frac{1}{|\lambda_1|^k}\right) = O\left(|\lambda_1|^{j-1-n_1+k}\frac{1}{|\lambda_1|^k}\right) = O(|\lambda_1|^{j-1-n_1}) = O\left(\frac{1}{|\lambda_1|^{n_1+1-j}}\right),$$

[5] It can be proved by mathematical induction.

then

$$\lim_{t\to\infty}|\tilde{e}_{x_j}(t)| = O\left(\frac{1}{|\lambda_1|^{n_1+1-j}}\right). \tag{A.14}$$

The order of the upper bounds given in (A.14) can provide some guide for GPI Observer's parameters design in practice. According to (A.14), the larger $|\lambda_1|$ is, the smaller the bound will be. Additionally, the bound order of the estimation error $\tilde{e}_{x_j}(t)$ with respect to $\tilde{e}_{x_{j+1}}(t)$ is $1/|\lambda_1|$, in particular, the ratio between the bound order of $\tilde{e}_{x_1}(t)$ (related to output estimation, $\hat{y}(t)$) and $\tilde{e}_{x_{n+1}}(t)$ (related to disturbance input estimation, $\hat{\xi}(t)$) is $1/|\lambda_1|^n$. □

Remark 3. Alternatively, the estimation errors bounds can be numerically obtained from (A.1)–(A.3), by computing their corresponding infinite norm.[6]

Remark 4. Consequently with the Theorem 1, the variables $\hat{x}_{n+1}$, $\hat{x}_{n+2},\ldots,\hat{x}_{n+m}$ track arbitrarily closely the unknown time functions, $\xi(t)$, and its time derivatives, $\xi^{(j)}(t)$, $j=1,\ldots,m-1$.

Remark 5. From (A.7) and given that the convolution operation is commutative the j-th estimation error can also be computed from $\tilde{e}_{x_j}(t) = \int_0^t g_j(t-\tau)\xi^{(m)}(\tau)\,d\tau$. For the case of $n+m$ real repeated eigenvalues, after a finite part integrations, one obtains $\int_0^t g_j(t-\tau)\xi^{(m)}(\tau)\,d\tau = -g_j(t)\xi^{(m-1)}(0) - \dot{g}_j(t)\xi^{(m-2)}(0) - \cdots - g_j^{(m-1)}(t)\xi(0) + \int_0^t \xi(\tau)g_j^{(m)}(t-\tau)\,d\tau$. $\tilde{e}_{x_j}(t)$. It is proven for this particular case that $\xi(t), \dot{\xi}(t),\ldots,\xi^{(m-1)}(t)$ must be bounded in $t=0$ in order to bound $\tilde{e}_{x_j}(t)$, this goes with Assumption A2.

Appendix B. Proof of Theorem 2

Proof. According to the Theorem 1, the term $\tilde{e}_{x_{n+1}}(t) = \xi(t) - \hat{x}_{n+1}(t)$ and the terms, $\tilde{e}_{x_k}(t)$, $k=1,2,\ldots,n$ all evolve in a small as desired neighborhood of zero. It follows that the right hand side of the linear system (10) evolves, in an uniformly ultimately bounded fashion, within a sufficiently small neighborhood of zero. Using the same arguments, in a dual context, as in the proof of Theorem 1, it follows that the tracking error $e_y(t)$ converges towards a small as desired vicinity of zero, provided the roots of $p_c(s)$ are located sufficiently to the left of the imaginary axis in $\mathbb{C}$. □

References

[1] Wu S-C, Tomizuka M. An iterative learning control design for self-servowriting in hard disk drives. Mechatronics 2010;20(1):53–8. http://dx.doi.org/10.1016/j.mechatronics.2009.06.004.

[2] Tayebi A, Abdul S, Zaremba M, Ye Y. Robust iterative learning control design: application to a robot manipulator. IEEE/ASME Trans Mechatron 2008;13(5):608–13. http://dx.doi.org/10.1109/TMECH.2008.2004627.

[3] Zhang B, Zhou K, Wang Y, Wang D. Performance improvement of repetitive controlled pwm inverters: a phase-lead compensation solution. Int J Circuit Theory Appl 2010;38:453–69. http://dx.doi.org/10.1002/cta.572.

[4] Gri nó R, Cardoner R, Costa-Castelló R, Fossas E. Digital repetitive control of a three-phase four-wire shunt active filter. IEEE Trans Ind Electron 2007;54(3):1495–503. http://dx.doi.org/10.1109/TIE.2007.894790.

[5] Houtzager I, van Wingerden J-W, Verhaegen M. Rejection of periodic wind disturbances on a smart rotor test section using lifted repetitive control. IEEE Trans Control Syst Technol 2013;21(2):347–59. http://dx.doi.org/10.1109/TCST.2011.2181171.

[6] Wang Y, Gao F, Doyle III FJ. Survey on iterative learning control, repetitive control, and run-to-run control. J Process Control 2009;19(10):1589–600. http://dx.doi.org/10.1029/2010JB000862.

[7] Li C, Zhang D, Zhuang X. A survey of repetitive control. In: Proceedings of the 2004 IEEE/RSJ international conference on intelligent robots and systems, vol. 2 (IROS 2004); 2004. p. 1160–6. http://dx.doi.org/10.1109/IROS.2004.1389553.

[8] Steinbuch M. Repetitive control for systems with uncertain period-time. Automatica 2002;38(12):2103–9. http://dx.doi.org/10.1016/S0005-1098(02)00134-6.

[9] Hu J-S. Variable structure digital repetitive controller. In: Proceedings of the American control conference; 1992. p. 2686–90.

[10] Steinbuch M, Weiland S, Singh T. Design of noise and period-time robust high-order repetitive control with application to optical storage. Automatica 2007;43(12):2086–95. http://dx.doi.org/10.1016/j.automatica.2007.04.011.

[11] Olm JM, Ramos GA, Costa-Castelló R. Adaptive compensation strategy for the tracking/rejection of signals with time-varying frequency in digital repetitive control systems. J Process Control 2010;20(4):551–8. http://dx.doi.org/10.1029/2010JB000862.

[12] Gao Z. Active disturbance rejection control: a paradigm shift in feedback control system design. In: American control conference; 2006. p. 7. http://dx.doi.org/10.1109/ACC.2006.1656579.

[13] Gao Z. On the centrality of disturbance rejection in automatic control. ISA Trans 2014; http://dx.doi.org/10.1016/j.isatra.2013.09.012. [in press].

[14] Zhao S. Gao Z. Modified active disturbance rejection control for time-delay systems. ISA Trans 2014; http://dx.doi.org/10.1016/j.isatra.2013.09.013 [in press].

[15] Ramírez-Neria M. Sira-Ramírez H. Garrido-Moctezuma R. Luviano-Juárez A. Linear active disturbance rejection control of underactuated systems: the case of the furuta pendulum, ISA Trans, 2014; http://dx.doi.org/10.1016/j.isatra.2013.09.023 [in press].

[16] Sira-Ramírez H, González-Monta nez F, Cortés-Romero J, Luviano-Juárez A. A robust linear field-oriented voltage control for the induction motor: experimental results. IEEE Trans Ind Electron 2013;60(8):3025–33. http://dx.doi.org/10.1109/TIE.2012.2201430.

[17] Sira-Ramírez H, Luviano-Juárez A, Cortés-Romero J. Control lineal robusto de sistemas no lineales. Rev Iberoam Autom Inf Ind 2011;8(1):14–28. http://dx.doi.org/10.1016/S1697-7912(11)70004-8.

[18] Francis B, Wonham WM. Internal model principle in control theory. Automatica 1976;12:457–65. http://dx.doi.org/10.1016/0005-1098(76)90006-6.

[19] Costa-Castelló R, Griñó R, Cardoner Parpal R, Fossas E. High-performance control of a single-phase shunt active filter. IEEE Trans Control Syst Technol 2009;17(6):1318–29. http://dx.doi.org/10.1109/TCST.2008.2007494.

[20] Inoue T. Practical repetitive control system design. In: Proceedings of the 29th IEEE conference on decision and control, vol. 3; 1990. p. 1673–8. http://dx.doi.org/10.1109/CDC.1990.203906.

[21] Tomizuka M. Dealing with periodic disturbances in controls of mechanical systems. Ann Rev Control 2008;32(2):193–9. http://dx.doi.org/10.1016/j.arcontrol.2008.07.002.

[22] Sira-Ramírez H, Agrawal SK. Differentially flat systems. New York: Marcel Dekker; 2004.

[23] Xue W, Huang Y. On performance analysis of adrc for nonlinear uncertain systems with unknown dynamics and discontinuous disturbances. In: 2013 32nd Chinese control conference (CCC); 2013. p. 1102–7.

[24] Gliklikh YE. Necessary and sufficient conditions for global-in-time existence of solutions of ordinary, stochastic, and parabolic differential equations. Abstr Appl Anal 2006;2006(1):17. http://dx.doi.org/10.1155/AAA/2006/39786.

[25] Ramos GA, Costa-Castelló R, Olm JM. Roto-magnet. Digital repetitive control under varying frequency conditions lecture notes in control and information sciences, vol. 446. Berlin, Heidelberg: Springer; 2013. p. 67–100. http://dx.doi.org/10.1007/978-3-642-37778-5_6.

[26] Xargay E, Costa-Castelló R. Modelado de una planta diseñada para ilustrar el principio del modelo interno. In: Somolinos J (Ed.), XXV jornadas de automática, ciudad real España; 2004. 9 pp.

[27] Parker G, Johnson C. Improved speed regulation and mitigation of drive-train torsion fatigue in flexible wind turbines, using disturbance utilization control: part 2. In: 41st Southeastern symposium on system theory (SSST 2009); 2009. p. 177–83. http://dx.doi.org/10.1109/SSST.2009.4806790.

[28] Freidovich L, Khalil H. Performance recovery of feedback-linearization-based designs. IEEE Trans Autom Control 2008;53(10):2324–34. http://dx.doi.org/10.1109/TAC.2008.2006821.

[29] Zhao S, Gao Z. An active disturbance rejection based approach to vibration suppression in two-inertia systems. In: American control conference (ACC), Baltimore, MD; 2010. p. 1520–5. http://dx.doi.org/10.1109/ACC.2010.5531284.

[30] Kim YC, Keel LH, Bhattacharyya S. Transient response control via characteristic ratio assignment. IEEE Trans Autom Control 2003;48(12):2238–44. http://dx.doi.org/10.1109/TAC.2003.820153.

[31] Precup R-E, Preitl S. Pi and pid controllers tuning for integral-type servo systems to ensure robust stability and controller robustness. Electr Eng 2006;88(2):149–56. http://dx.doi.org/10.1007/s00202-004-0269-8.

[32] Ginter V, Pieper J. Robust gain scheduled control of a hydrokinetic turbine. IEEE Trans Control Syst Technol 2011;19(4):805–17. http://dx.doi.org/10.1109/TCST.2010.2053930.

[33] Jin QB, Liu Q. Imc-pid design based on model matching approach and closed-loop shaping. ISA Trans 2014;53(2):462–73. http://dx.doi.org/10.1016/j.isatra.2013.11.005.

[34] Skogestad S, Postlethwaite I. Multivariable feedback control: analysis and design. 2nd ed.. New York: John Wiley; 2005.

[6] Infinite norm of $G(s)$ calculated as $\|G(s)\|_\infty = \max_\omega |G(j\omega)|$.